JACS
JOURNAL OF THE AMERICAN CHEMICAL SOCIETY

Communication

pubs.acs.org/JACS

Semiconducting Polymer Nanobioconjugates for Targeted Photothermal Activation of Neurons

Yan Lyu,[†,§] Chen Xie,[†,§] Svetlana A. Chechetka,[‡] Eijiro Miyako,[*,‡] and Kanyi Pu[*,†]

[†]School of Chemical and Biomedical Engineering, Nanyang Technological University, Singapore 637457, Singapore

[‡]Department of Materials and Chemistry, Nanomaterial Research Institute (NMRI), National Institute of Advanced Industrial Science and Technology (AIST), Central 5, 1-1-1 Higashi, Tsukuba, Ibaraki 305-8565, Japan

Supporting Information

ABSTRACT: Optogenetics provides powerful means for precise control of neuronal activity; however, the requirement of transgenesis and the incapability to extend the neuron excitation window into the deep-tissue-penetrating near-infrared (NIR) region partially limit its application. We herein report a potential alternative approach to optogenetics using semiconducting polymer nanobioconjugates ($SPNs_{bc}$) as the photothermal nanomodulator to control the thermosensitive ion channels in neurons. $SPNs_{bc}$ are designed to efficiently absorb the NIR light at 808 nm and have a photothermal conversion efficiency higher than that of gold nanorods. By virtue of the fast heating capability in conjunction with the precise targeting to the thermosensitive ion channel, $SPNs_{bc}$ can specifically and rapidly activate the intracellular Ca^{2+} influx of neuronal cells in a reversible and safe manner. Our study provides an organic nanoparticle based strategy that eliminates the need for genetic transfection to remotely regulate cellular machinery.

Spatial and temporal regulation of cellular activity is imperative to decipher underlying physiological processes and develop novel therapeutic modalities. Optogenetics combines optical methods with molecular genetics, providing a powerful means for precise control of defined events in specific cells of living tissues.[1] In particular, microbial opsins such as channel-rhodopsin and halo-rhodopsin are selectively expressed in the targeted neuronal cells, allowing light to control the relevant ion channel and subsequently activate neuronal activity.[2] With the advantage of simultaneous input−output interrogation of neurons that is not accessible for electrical stimulation, optogenetics has opened new landscapes for neuroscience.[3] However, because microbial opsins and their variants can only absorb the light ranging from ∼470 to 630 nm,[4] current optogenetics methods are limited to the visible light spectrum that has a shallow depth of tissue penetration. Although upconversion nanoparticles can help shift the neuron excitation window to near-infrared (NIR) region,[5] the requirement for transgenesis still complicates the implementation of optogenetics and partially constrains its application.

One emerging alternative to optogenetics is the nanoparticle-based direct thermal stimulation of unmodified neurons.[6−12] Magnetic iron oxide nanoparticles and optical metallic nanoparticles can respectively convert low-radiofrequency alternating magnetic fields and photon energy into heat,[13,14] giving rise to increased local temperature. Such a nanoparticle-mediated temperature change can be transduced by a thermosensitive protein channel into cellular responses. However, probably due to the slow magnetothermal generation, magnetic iron oxide nanoparticles required tens to thousands of seconds to induce increased calcium ion (Ca^{2+}) influx, which exceeded temporal dynamics of neuronal firing.[6,7] In comparison, photothermal stimulation based on gold nanoparticles or carbon nanotubes showed relatively shorter activation time (∼30 s).[9,10] However, current methods primarily relied on the electrostatic or hydrophobic interactions between metallic nanoparticles and plasma membrane,[9,10] which performed nonspecifically and had the risk of damaging cellular membrane and causing cytotoxicity. Thereby, selective and rapid activation of specific thermosensitive channels of unmodified neuron remains to be demonstrated.

In this study, we report the design and synthesis of semiconducting polymer nanobioconjugates ($SPNs_{bc}$) with high photothermal conversion efficiency and demonstrate their proof-of-concept application in specific photothermal activation of neurons by targeting transient receptor potential cation channel subfamily V member 1 (TRPV1). TRPV1 is an ion permeable polymodal channel that can be activated by exogenous and endogenous physical and chemical stimuli such as heat.[14] TRPV1 is widely expressed across the mammalian nervous system and thus serves as an intrinsic thermosensitive channel for us to precisely control the Ca^{2+} influx in neuronal cells. Semiconducting polymer nanoparticles (SPNs) are chosen as the photothermal nanomodulator to remotely increase the local temperature and subsequently activate TRPV1. Because SPNs are transformed from semiconducting polymers (SPs) that are completely organic and biologically inert, they circumvent the issue of heavy metal ion-induced toxicity to living organisms and possess good biocompatibility.[15,16] In addition to molecular imaging applications, we recently revealed that SPNs can convert photon energy into heat, permitting sensitive photoacoustic imaging and efficient photothermal therapy of tumors.[17] However, to fulfill their function in photothermal stimulation of neuronal cells, development of SPNs with high photothermal conversion efficiency is essential.

To align the photothermal features of SPNs with NIR laser at 808 nm that has deep-tissue penetration,[18] a new polymer, poly(cyclopentadithiophene-*alt*-diketopyrrolopyrrole) (SP2),

Received: May 20, 2016
Published: July 12, 2016

DOI: 10.1021/jacs.6b05192
J. Am. Chem. Soc. 2016, 138, 9049−9052

was designed and synthesized via Stille polymerization between monomers 1 and 2. Different from its analogue poly(cyclopentadithiophene-*alt*-benzothiadiazole) (SP1, Figure 1b), SP2 had the structure unit of diketopyrrolopyrrole in the

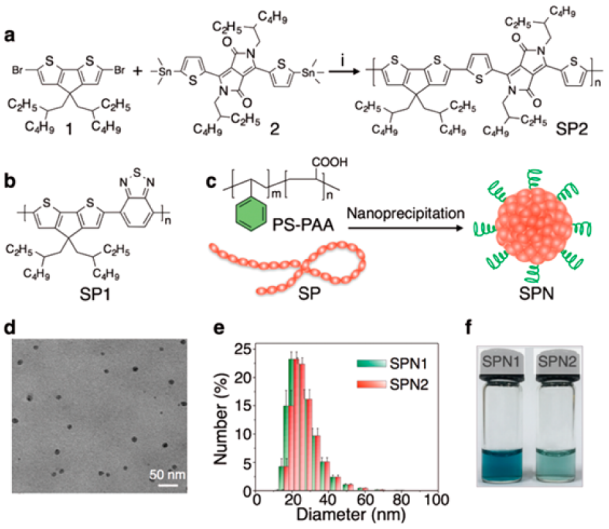

Figure 1. Synthesis and characterization of SPNs. (a) Synthetic route of SP2 via Stille polymerization under the reaction conditions (i) $PdCl_2(PPh_3)_2$ and 2,6-di-*tert*-butylphenol, 100 °C for 12 h. (b) Chemical structures of SP1. (c) Schematic illustration of synthesis of SPNs. (d) Representative TEM image of SPNs: SPN2. (e) Representative DLS profiles of SPNs. (f) Photos of SPN solutions (18 μg mL^{-1}).

backbone that narrowed down the band gap, shifting the absorption into the NIR region. SP1 and SP2 were respectively transformed into water-soluble nanoparticles via nanocoprecipitation with polystyrene-*b*-poly(acrylic acid) (PS-PAA) (Figure 1c). This amphiphilic copolymer conferred SPNs with not only good water-solubility but also the carboxyl groups on the surface for postbioconjugation. The SPNs had uniform spherical morphology with the hydrodynamic diameters of ~25 nm (Figures 1d,e). The nanoparticle solutions were clear (Figure 1f) and remained stable for months with no obvious change in size (Figure S2, Supporting Information).

The optical and photothermal properties of SPNs were studied and compared with the polyethylene glycol (PEG) coated gold nanorod (GNRs). Due to the enhanced charge transfer, the maximum absorption of SPN2 was red-shifted by 100 to 766 nm relative to that of SPN1 (660 nm) (Figure 2a). GNR had the maximum at 780 nm, serving as a fair control for SPN2. The peak mass extinction coefficient of SPN2 was 87 cm^{-1} mg^{-1} mL, similar to that of SPN1 (90 cm^{-1} mg^{-1} mL) but 4.35-fold larger than that of GNR (20 cm^{-1} mg^{-1} mL). Under continuous laser irradiation at 808 nm, all the nanoparticles showed gradually increased solution temperatures and reached plateau at t = 360 s (Figure 2b). At each time point, the temperature of SPN2 was higher than others, indicating its faster heating capability. The maximum photothermal temperature that SPN2 could reach was 70 °C, which was ~1.4-fold higher than those of SPN1 and GNR (Figure 2c). The maximum temperature of GNR (50 °C) was similar to that of other gold nanostructures reported previously,[19] implying that SPN2 could be a relatively better photothermal agent on a per mass basis.

The photothermal conversion efficiency of SPN2 at 808 nm was calculated to be 20%, 1.18-fold higher than that of GNR

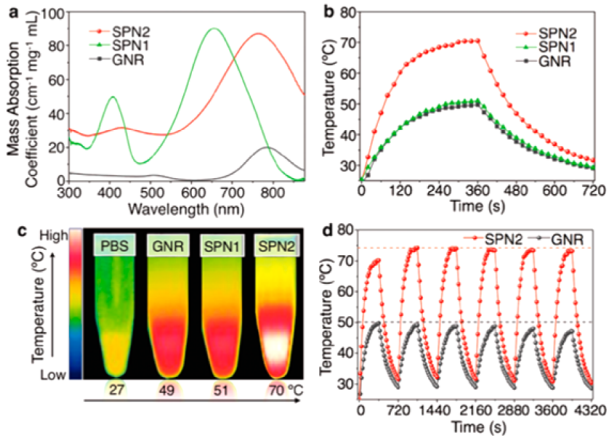

Figure 2. Optical and photothermal characterization of SPNs. (a) Absorption of SPNs and GNR. (b) Temperatures of SPN and GNR solutions as a function of laser irradiating time. (c) Thermal images of SPNs and GNR at their respective maximum temperatures. (d) Stability study of SPN2 and GNR under the photothermal heating and natural cooling cycles. The concentrations of nanoparticles were 18 μg mL^{-1} in 1× PBS (pH = 7.4). The laser irradiation wavelength was at 808 nm with a power of 1 W cm^{-2}.

(17%) but 1.5-fold lower than that of SPN1 (30%). Thereby, the order of the maximum photothermal temperatures (SPN2 > SPN1 ≈ GNR) was not solely determined by the order of their photothermal conversion efficiencies (SPN1 > SPN2 > GNR); rather, it was more affected by their mass extinction coefficients at 808 nm. The photothermal stability was studied by reversibly heating and cooling the nanoparticle solutions (Figure 2d). SPN2 exhibited slightly increased maximum temperature after the first heating cycle because the solution did not completely cool back to the room temperature before the new heating cycle. Nevertheless, the maximum temperatures of SPN2 remained nearly the same for at least 5 cycles. In contrast, GNR exhibited gradually decreased maximum temperature due to their susceptibility to laser-induced deformation.[20] Thereby, these data verified that SPN2 had higher photothermal conversion efficiency, faster heating capability, and better photothermal stability as compared with GNR.

To specifically activate the thermosensitive ion channels of neurons, SPNs were conjugated with anti-TRPV1 antibody via a carbodiimide coupling reaction between the carboxyl group of SPNs and the amine group of anti-TRPV1 antibody (Figure 3a). The agarose gel electrophoresis revealed that $SPN1_{bc}$ migrated much less as compared with SPN1 (Figure 3b). Additionally, DLS showed that the resulting $SPN1_{bc}$ exhibited increased hydrodynamic diameter from 25 to 37 nm (Figure 3c). The zeta potential of $SPN1_{bc}$ was −14.73 ± 0.84 eV, higher than that of SPN1 (−17.77 ± 1.69 eV). These changes implied that anti-TRPV1 antibody was successfully conjugated on the nanoparticle surface.

Because $SPN1_{bc}$ was fluorescent with the emission maximum at 838 nm (Figure S3, Supporting Information), the targeting capability of $SPN1_{bc}$ was examined using fluorescence cell imaging. Mouse neuroblastoma/rat dorsal root ganglion (DRG) neuron hybrid ND7/23 cells that intrinsically express TRPV1 on their plasma membrane were chosen as the example neural cells, while human cervical carcinoma HeLa cells were used as the TRPV1 negative control. After incubation with $SPN1_{bc}$ and multiple washing steps to remove the free nanoparticles, live-cell imaging was conducted. Red fluorescence around the cell

DOI: 10.1021/jacs.6b05192
J. Am. Chem. Soc. 2016, 138, 9049−9052

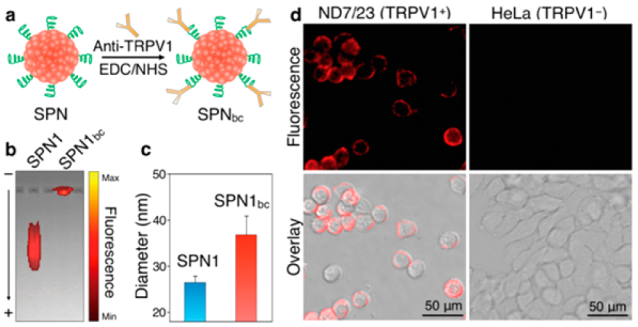

Figure 3. Synthesis and characterization of $SPNs_{bc}$. (a) Synthesis of $SPNs_{bc}$ via 1-ethyl-3-(3-(dimethylamino)propyl)carbodiimide (EDC)/*N*-hydroxysuccinimide (NHS) coupling reaction. (b) Agarose gel electrophoresis of SPN1 and $SPN1_{bc}$. (c) Hydrodynamic diameters of SPN1 and $SPN1_{bc}$. (d) Fluorescence cell images of mouse neuroblastoma/DRG neuron hybrid ND7/23 cells and Hela cells treated with $SPN1_{bc}$. Cy5 channel was used to excite the cells, and fluorescence signals were detected at 725 ± 50 nm.

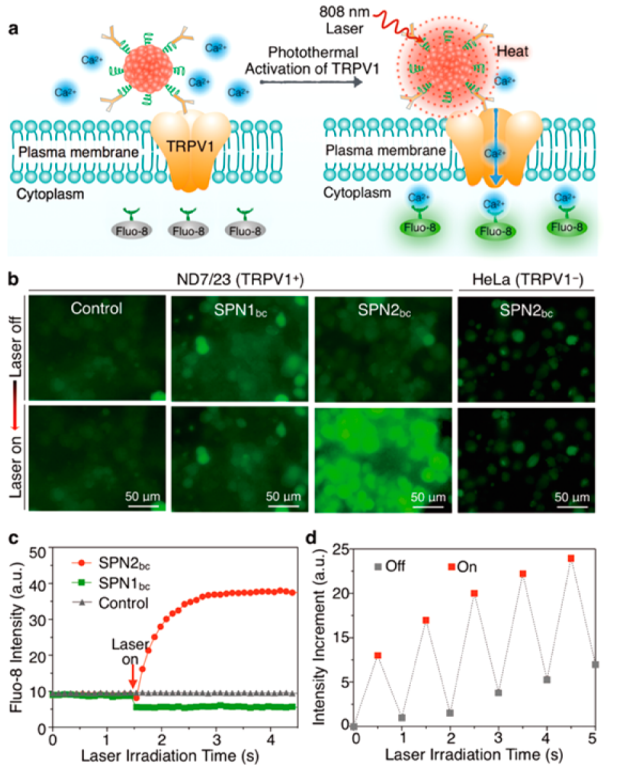

Figure 4. NIR photothermal activation of the TRPV1 ion channels in mouse neuroblastoma/DRG neuron hybrid ND7/23 cells. (a) Schematic illustration of SPN_{bc} controlled photothermal activation of Ca^{2+} channels in neurons. The intracellular concentration of Ca^{2+} was monitored in real-time by using Fluo-8 as the indicator, which turned on its fluorescence upon binding with Ca^{2+}. (b) Fluorescence images of ND7/23 or HeLa treated with $SPN1_{bc}$ or $SPN2_{bc}$ before and after laser irradiation time at 808 nm (104 $\mu W\ \mu m^{-2}$) for 2 s. (c) The fluorescence intensity of Fluo-8 as a function of laser irradiation time. (d) Changes in the fluorescence intensity of Fluo-8 with the laser irradiation at 808 nm switching on and off at an interval of 0.5 s.

periphery was detected for ND7/23 cells; in contrast, no fluorescence was visible for HeLa cells under the same experimental conditions because of the negatively charged surface of $SPN1_{bc}$ that prevented nonspecific cellular uptake.[15] Thereby, the fluorescence imaging data clearly confirmed that $SPN1_{bc}$ effectively bound to the TRPV1 ion channels intrinsically expressed on the plasma membrane of DRG neurons. This ensured that the localized heat from the SPN_{bc} nanomodulator could be quickly dissipated to the TRPV1 ion channels, showing the feasibility of specific photothermal activation of neuronal activity.

The ability of $SPNs_{bc}$ to activate TRPV1 was evaluated using mouse neuroblastoma/rat DRG neuron hybrid ND7/23 cells and HeLa cells as the TRPV1 positive and the negative cells, respectively. The Ca^{2+} influx, as a vital biological process in neurotransmitter release,[21] was monitored in real-time using a fluorescent turn-on intracellular indicator (Fluo-8) (Figure 4a). Without nanoparticle treatment, no fluorescence intensity increase of Fluo-8 was observed for ND7/23 cells after irradiation at 808 nm for 3 s, proving that the laser irradiation alone was unable to activate the TRPV1 ion channels under our experimental conditions. In contrast, a significant increase in the fluorescence intensity of Fluo-8 was observed for $SPN2_{bc}$-treated but not for $SPN1_{bc}$-treated ND7/23 cells (Figure 4b). This should be ascribed to the faster heating capability of $SPN2_{bc}$ relative to $SPN1_{bc}$ as observed in solution (Figure 2b). Accordingly, $SPN2_{bc}$ was able to quickly increase the local temperature of TRPV1 above the threshold (43 °C) to activate the TRPV1 ion channels, inducing the intracellular Ca^{2+} influx; this was not possible for $SPN1_{bc}$ even with the longer laser irradiation time. Such a SPN-dependent activation highlighted the importance of molecular design of SP for photothermal applications. The fact that $SPN2_{bc}$ could not induce the change in the fluorescence of HeLa cells further confirmed that the observed fluorescence enhancement resulted from the photothermal activation of TRPV1 ion channels. These findings reflected that the cellular membrane of HeLa cells remained intact under laser irradiation; otherwise, membrane disruption could occur, leading to nonspecific Ca^{2+} influx and consequently increased fluorescence.[9] In fact, the cell viability assays verified that SPNs had good cytocompatibility and that there was no cytotoxicity induced by such a short laser irradiation process (Figures S4 and S5, Supporting Information). The biosafety of $SPN2_{bc}$-mediated photothermal activation of neuronal cells should benefit from the efficient photothermal conversion of SPN2 that minimized the laser irradiation time and reduces the probability of noxious heat.

To determine whether SPN_{bc} had the capability for simultaneous input−output interrogation of neuronal cells, monitoring of Fluo-8 fluorescence was conducted in real time along with photothermal stimulation by $SPNs_{bc}$. As soon as the laser irradiation initiated, Fluo-8 fluorescence immediately increased until its plateau at ∼1.5 s for $SPN2_{bc}$-treated ND7/23 cells (Figure 4c); this was not observed for both $SPN1_{bc}$-treated and untreated cells. Due to the limited temporal resolution of the fluorescence microscopy used, the first data point collected was at 100 ms after laser irradiation. At this time point, the fluorescence intensity of Fluo-8 already increased by 2-fold, implying the instant occurrence of intracellular Ca^{2+} influx upon laser irradiation. This phenomenon verified that the SPN_{bc}-based photothermal approach activated neurons within milliseconds. In addition, the TRPV-1 Ca^{2+} channels could be reversibly activated and silenced by switching the laser irradiation on and off at an interval of 0.5 s (Figure 4d and Figure S6, Supporting Information). These data not only demonstrated the capability of simultaneous input−output interrogation of neuronal cells within milliseconds but also highlight the instant

DOI: 10.1021/jacs.6b05192
J. Am. Chem. Soc. 2016, 138, 9049−9052

photothermal stimulation of neuronal cells as a result of rapid heating capability of SPN2.

In conclusion, we have designed and synthesized NIR-absorbing organic SPNs with the higher photothermal conversion efficiency, faster heating capability, and better photothermal stability as compared with GNR and demonstrated the application in the specific thermal stimulation of neurons without genetic transfection of microbial opsins. The surface amenability of SPNs enabled efficient conjugation with anti-TRPV1 antibody, leading to smart photothermal bioconjugates ($SPNs_{bc}$) that precisely targeted the thermosensitive TRPV1 ion channels on the plasma membrane of neurons. The high photothermal performance and the targeting capability minimized the stimulation time and avoided the off-target side effect, respectively, both of which contributed to reduced probability of noxious heat to living cells. Upon transient NIR laser irradiation at 808 nm, SPN_{bc} acted as a wireless remote nanomodulator to rapidly and specifically activate the TRPV1 ion channels, inducing the intracellular Ca^{2+} influx of neurons within milliseconds in a safe and reversible manner.

To the best of our knowledge, our study provides the first example of an organic nanoparticle based photothermal system for precise control of defined events in neurons; this system could represent a potential alternative to optogenetics. Other organic biophotonic nanoparticles such as porphysomes and frozen micellar naphthalocyanines can also be tailored for such application.[22] In addition to providing insights into fundamental neuroscience, the structural flexibility of SPNs will facilitate the development of novel therapeutic approaches such as photothermic regulation of gene therapy and photothermal therapy of astrocytoma that has intrinsically expressed TRPV1.

■ ASSOCIATED CONTENT

Supporting Information

The Supporting Information is available free of charge on the ACS Publications website at DOI: 10.1021/jacs.6b05192.

Detailed experiment procedures and supporting figures (PDF)

■ AUTHOR INFORMATION

Corresponding Authors

*e-miyako@aist.go.jp

*kypu@ntu.edu.sg

Author Contributions

§These authors contributed equally to this work.

Notes

The authors declare no competing financial interest.

■ ACKNOWLEDGMENTS

This work was supported by Nanyang Technological University start-up grant (NTU-SUG: M4081627.120), Academic Research Fund Tier 1 from Singapore Ministry of Education (M4011559.120, RG133/15), a Japan Society for the Promotion of Science (JSPS) KAKENHI Grant-in-Aid for Scientific Research (B) (16H03834), and a JSPS KAKENHI Grant-in-Aid for Challenging Exploratory Research (16K13632).

■ REFERENCES

(1) Deisseroth, K. *Nat. Methods* **2011**, *8*, 26−29.

(2) Zhang, K.; Cui, B. *Trends Biotechnol.* **2015**, *33*, 92−100.

(3) Fenno, L.; Yizhar, O.; Deisseroth, K. *Annu. Rev. Neurosci.* **2011**, *34*, 389−412.

(4) Lin, J. Y.; Knutsen, P. M.; Muller, A.; Kleinfeld, D.; Tsien, R. Y. *Nat. Neurosci.* **2013**, *16*, 1499−1508.

(5) Wu, X.; Zhang, Y.; Takle, K.; Bilsel, O.; Li, Z.; Lee, H.; Zhang, Z.; Li, D.; Fan, W.; Duan, C.; Chan, E. M.; Lois, C.; Xiang, Y.; Han, G. *ACS Nano* **2016**, *10*, 1060−1066.

(6) Huang, H.; Delikanli, S.; Zeng, H.; Ferkey, D. M.; Pralle, A. *Nat. Nanotechnol.* **2010**, *5*, 602−606.

(7) Stanley, S. A.; Gagner, J. E.; Damanpour, S.; Yoshida, M.; Dordick, J. S.; Friedman, J. M. *Science* **2012**, *336*, 604−608.

(8) Chen, R.; Romero, G.; Christiansen, M. G.; Mohr, A.; Anikeeva, P. *Science* **2015**, *347*, 1477−1480.

(9) Nakatsuji, H.; Numata, T.; Morone, N.; Kaneko, S.; Mori, Y.; Imahori, H.; Murakami, T. *Angew. Chem., Int. Ed.* **2015**, *54*, 11725−11729.

(10) Miyako, E.; Russier, J.; Mauro, M.; Cebrián, C.; Yawo, H.; Ménard-Moyon, C.; Hutchison, J. A.; Yudasaka, M.; Iijima, S.; De Cola, L.; Bianco, A. *Angew. Chem., Int. Ed.* **2014**, *53*, 13121−13125.

(11) Zhang, Y.; Huang, L.; Li, Z.; Ma, G.; Zhou, Y.; Han, G. *ACS Nano* **2016**, *10*, 3881−3885.

(12) Yu, J.; Yang, C.; Li, J.; Ding, Y.; Zhang, L.; Yousaf, M. Z.; Li, J.; Pang, R.; Wei, L.; Xu, L.; Sheng, F.; Li, C.; Li, G.; Zhao, L.; Hou, Y. *Adv. Mater.* **2014**, *26*, 4114−4120.

(13) Cheng, K.; Kothapalli, S. − R.; Liu, H.; Koh, A. L.; Jokerst, J. V.; Jiang, H.; Yang, M.; Li, J.; Levi, J.; Wu, J. C.; Gambhir, S. S.; Cheng, Z. *J. Am. Chem. Soc.* **2014**, *136*, 3260−3571.

(14) Tominaga, M.; Caterina, M. J.; Malmberg, A. B.; Rosen, T. A.; Gilbert, H.; Skinner, K.; Raumann, B. E.; Basbaum, A. I.; Julius, D. *Neuron* **1998**, *21*, 531−543.

(15) Wu, C.; Chiu, D. T. *Angew. Chem., Int. Ed.* **2013**, *52*, 3086−3109.

(16) Zhu, C. L.; Liu, L. B.; Yang, Q.; Lv, F. T.; Wang, S. *Chem. Rev.* **2012**, *112*, 4687−4735.

(17) (a) Pu, K.; Shuhendler, A. J.; Jokerst, J. V.; Mei, J.; Gambhir, S. S.; Bao, Z.; Rao, J. *Nat. Nanotechnol.* **2014**, *9*, 233−239. (b) Lyu, Y.; Fang, Y.; Miao, Q.; Zhen, X.; Ding, D.; Pu, K. *ACS Nano* **2016**, *10*, 4472−4481. (c) Miao, Q.; Lyu, Y.; Ding, D.; Pu, K. *Adv. Mater.* **2016**, *28*, 3662−3668. (d) Pu, K.; Mei, J.; Jokerst, J. V.; Hong, G.; Antaris, A. L.; Chattopadhyay, N.; Shuhendler, A. J.; Kurosawa, T.; Zhou, Y.; Gambhir, S. S.; Bao, Z.; Rao, J. *Adv. Mater.* **2015**, *27*, 5184−5190.

(18) Mitsunaga, M.; Ogawa, M.; Kosaka, N.; Rosenblum, L. T.; Choyke, P. L.; Kobayashi, H. *Nat. Med.* **2011**, *17*, 1685−1691.

(19) (a) Wang, Y.; Black, K. C. L.; Luehmann, H.; Li, W.; Zhang, Y.; Cai, X.; Wan, D.; Liu, S. − Y.; Li, M.; Kim, P.; Li, Z. Y.; Wang, L. H. V.; Liu, Y.; Xia, Y. *ACS Nano* **2013**, *7*, 2068−2077. (b) Kumar, A.; Kumar, S.; Rhim, W. K.; Kim, G. H.; Nam, J. M. *J. Am. Chem. Soc.* **2014**, *136*, 16317−16325.

(20) Link, S.; Burda, C.; Nikoobakht, B.; El-Sayed, M. A. *J. Phys. Chem. B* **2000**, *104*, 6152−6163.

(21) Alberts, B.; Bray, D.; Hopkin, K.; Johnson, A.; Lewis, J.; Raff, M.; Roberts, K.; Walter, P. *Essential Cell Biology*, 3rd ed.; Garland: New York, 2009.

(22) (a) Zhang, Y.; Jeon, M.; Rich, L. J.; Hong, H.; Geng, J.; Zhang, Y.; Shi, S.; Barnhart, T. E.; Alexandridis, P.; Huizinga, J. D.; Seshadri, M.; Cai, W.; Kim, C.; Lovell, J. F. *Nat. Nanotechnol.* **2014**, *9*, 631−638. (b) Huynh, E.; Leung, B. Y. C.; Helfield, B. L.; Shakiba, M.; Gandier, J.; Jin, C. S.; Master, E. R.; Wilson, B. C.; Goertz, D. E.; Zheng, G. *Nat. Nanotechnol.* **2015**, *10*, 325−332.

DOI: 10.1021/jacs.6b05192
J. Am. Chem. Soc. 2016, 138, 9049−9052